



Long-term Particulate Matter Modeling for Health Effects Studies in California – Part II: Concentrations and Sources of Ultrafine Organic Aerosols

Jianlin Hu^{1*}, Shantanu Jathar², Hongliang Zhang³, Qi Ying⁴, Shu-Hua Chen⁵, Christopher D. Cappa⁶,
and Michael J. Kleeman^{6*}

¹Jiangsu Key Laboratory of Atmospheric Environment Monitoring and Pollution Control, Jiangsu
Engineering Technology Research Center of Environmental Cleaning Materials, Collaborative
Innovation Center of Atmospheric Environment and Equipment Technology, School of Environmental
Science and Engineering, Nanjing University of Information Science & Technology, 219 Ningliu Road,
Nanjing 210044, China

²Department of Mechanical Engineering, Colorado State University, Fort Collins CO, USA

³Department of Civil and Environmental Engineering, Louisiana State University, Baton Rouge LA, USA

⁴Zachry Department of Civil Engineering, Texas A&M University, College Station TX, USA

⁵Department of Land, Air, and Water Resources, University of California, Davis. One Shields Avenue,
Davis, CA, USA

⁶Department of Civil and Environmental Engineering, University of California, Davis. One Shields
Avenue, Davis CA, USA

*Corresponding authors:

Jianlin Hu, Tel.: +86 25 5873 1504; E-mail address: jianlinhu@nuist.edu.cn; hu_jianlin@126.com

Michael J. Kleeman, Tel.: +1 530 752 8386; fax; +1 530 752 7872. E-mail address:

mjkleeman@ucdavis.edu



1 Abstract

2 Organic aerosol (OA) is a major constituent of ultrafine particulate matter ($PM_{0.1}$).
3 Recent epidemiological studies have identified associations between $PM_{0.1}$ OA and premature
4 mortality and low birth weight. In this study, the source-oriented UCD/CIT model was used to
5 simulate the concentrations and sources of primary organic aerosols (POA) and secondary
6 organic aerosols (SOA) in $PM_{0.1}$ in California for a 9-year (2000 - 2008) modeling period with 4
7 km horizontal resolution to provide more insights about $PM_{0.1}$ OA for health effects studies. As a
8 related quality control, predicted monthly average concentrations of fine particulate matter
9 ($PM_{2.5}$) total organic carbon at six major urban sites had mean fractional bias of -0.31 to 0.19 and
10 mean fractional errors of 0.4 to 0.59. The predicted ratio of $PM_{2.5}$ SOA/OA was lower than
11 estimates derived from chemical mass balance (CMB) calculations by a factor of 2~3, which
12 suggests the potential effects of processes such as POA volatility, additional SOA formation
13 mechanism, and missing sources. OA in $PM_{0.1}$, the focus size fraction of this study, is dominated
14 by POA. Wood smoke is found to be the single biggest source of $PM_{0.1}$ OA in winter in
15 California, while meat cooking, mobile emissions (gasoline and diesel engines), and other
16 anthropogenic sources (mainly solvent usage and waste disposal) are the most important sources
17 in summer. Biogenic emissions are predicted to be the largest $PM_{0.1}$ SOA source, followed by
18 mobile sources and other anthropogenic sources, but these rankings are sensitive to the SOA
19 model used in the calculation. Air pollution control programs aiming to reduce the $PM_{0.1}$ OA
20 concentrations should consider controlling solvent usage, waste disposal, and mobile emissions
21 in California, but these findings should be revisited after the latest science is incorporated into
22 the SOA exposure calculations. The spatial distributions of SOA associated with different
23 sources are not sensitive to the choice of SOA model, although the absolute amount of SOA can



24 change significantly. Therefore, the spatial distributions of $PM_{0.1}$ POA and SOA over the 9-year
25 study period provide useful information for epidemiological studies to further investigate the
26 associations with health outcomes.

27

28 **Key Words:** Primary organic aerosols, secondary organic aerosols, California, sources,
29 UCD/CIT model.

30



31 1. Introduction

32 Organic aerosol (OA) is a significant constituent of fine particulate matter ($PM_{2.5}$) (Zhang
33 et al., 2007) and a dominant constituent of ultrafine particulate matter ($PM_{0.1}$) (Kleeman et al.,
34 2009; Sardar et al., 2005a). Epidemiology studies carried out over the past 20 years link $PM_{2.5}$ to
35 severe short-term and long-term health effects such as asthma, cardio-respiratory disease, and
36 lung cancer (Dockery, 2001; Dockery and Pope, 1994; Dockery et al., 1993; Franklin et al., 2007;
37 Le Tertre et al., 2002; Pope et al., 2002; Pope and Dockery, 2006). Epidemiological studies for
38 $PM_{0.1}$ mass are in the early stages of development but preliminary results show associations with
39 premature mortality (Ostro et al., 2015) and low birth weight (Laurent et al., 2014). OA is an
40 important species due to its contribution to $PM_{2.5}$ and $PM_{0.1}$ mass, and the toxicity of some
41 compounds within OA has motivated even greater scrutiny in health studies (Mauderly and
42 Chow, 2008). A few $PM_{2.5}$ epidemiology studies have investigated the associations between
43 exposure to OA and health effects with mixed results (Cao et al., 2012; Krall et al., 2013; Levy et
44 al., 2012; Mar et al., 2000; Ostro et al., 2006; Ostro et al., 2010). The early epidemiological
45 studies conducted for $PM_{0.1}$ have identified subcategories of OA that are highly associated with
46 negative health effects (Laurent et al., 2016a; Laurent et al., 2014; Laurent et al., 2016b; Ostro et
47 al., 2015) and these results merit further investigation to identify the exact sources and
48 compound classes that may be related to $PM_{0.1}$ OA toxicity.

49 The exposure fields used in the published $PM_{0.1}$ epidemiology studies to date have been
50 generated with chemical transport models (CTMs) because $PM_{0.1}$ measurements with sufficient
51 spatial or temporal resolution are not widely available. In these studies, predictions using the
52 UCD/CIT (University of California Davis/California Institute of Technology) model were
53 evaluated against $PM_{2.5}$ and $PM_{0.1}$ point measurements as a confidence building exercise and the



54 model predictions were then used to estimate exposure fields with ~4km and ~24hr resolution
55 over the state of California (Hu et al., 2014a; Hu et al., 2014b; Hu et al., 2015). The OA exposure
56 fields generated through this approach reflect the state-of-the-science predictions from CTMs at
57 the time they were done, but they may not capture the full complexity of atmospheric OA. OA
58 consists of primary organic aerosol (POA) and secondary organic aerosol (SOA). POA is directly
59 emitted to the atmosphere in the particle phase and SOA is formed in the atmosphere from the
60 oxidation of volatile or semi-volatile organic compounds (Seinfeld and Pankow, 2003). Both
61 POA and the precursors of SOA can be emitted from anthropogenic and biogenic sources
62 (Mauderly and Chow, 2008). Numerous theories have been put forward about the volatility of
63 POA (Robinson et al., 2007), the conversion of intermediate volatility compounds to SOA
64 (Jathar et al., 2014; Zhao et al., 2014), and the role of water in SOA formation (Jathar et al., 2016;
65 Pankow et al., 2015). A comprehensive model for OA that has been fully constrained by
66 measurements has not been demonstrated to date, which makes it difficult to estimate $PM_{2.5}$ OA
67 exposure using CTMs. However, measurements indicate the OA in the $PM_{0.1}$ size fraction is
68 more heavily influenced by POA (Ham and Kleeman, 2011; Kleeman et al., 2009), which makes
69 estimating exposure to $PM_{0.1}$ using CTMs more feasible.

70 The current paper, as the fourth in the series (Hu et al., 2014a; Hu et al., 2014b; Hu et al.,
71 2015), investigates the UCD/CIT model capability in predicting the concentrations and sources
72 of POA and SOA in $PM_{0.1}$. The objective of this study is to identify the features of the CTM
73 POA and SOA results that could add skill to the exposure assessment for epidemiological studies
74 and to discuss the potential problems in modeling POA and SOA for use in health effects studies.

75



76 2. Methods

77 2.1 Model Description

78 The source-oriented University of California-Davis/California Institute of Technology
79 (UCD/CIT) air quality model was used to predict OA concentrations in the current study. The
80 UCD/CIT model tracks primary particles and SOA formation from different sources separately
81 through the calculation of all major aerosol processes such as emissions, transport, deposition,
82 gas-to-particle conversion, and coagulation. The standard algorithms of these processes used in
83 the current study are provided in a companion paper (Hu et al., 2015) and references therein,
84 therefore only the details of the algorithms for POA and SOA source apportionment calculation
85 are described here.

86 The UCD/CIT source-oriented air quality model tracks primary particles emitted from
87 different sources by adding artificial tracers to represent total primary mass contributions from
88 different sources in each particle size bin (Ying et al., 2008). The emissions of tracers are
89 empirically set to be 1% of the total mass of primary particles emitted from each source category,
90 thus the particle radius and the dry deposition rate are not significantly changed. The primary PM
91 total mass concentrations from a given source then are directly correlated with the simulated
92 artificial tracer concentrations from that source. Source specific emission profiles are used to
93 estimate the POA concentrations in the primary PM total mass using the equation (1):

$$94 \quad \text{POA}_{i,j} = C_{i,j} \times A_{i,j} \quad (\text{eq. 1})$$

95 where $\text{POA}_{i,j}$ and $C_{i,j}$ represent POA concentration and primary PM total mass concentration in
96 size bin i from j th source, respectively. $A_{i,j}$ represents OA fraction per unit mass of PM emitted
97 from the j th emission source in size bin i . More details describing the POA source apportionment



98 technique and the emission profiles are provided in the previous studies (Ying and Kleeman,
99 2004; Ying et al., 2008).

100 The SOA module used in the current study follows the two-product method described by
101 Carlton et al. (2010). SOA formation is considered from seven precursors: isoprene,
102 monoterpenes, sesquiterpenes, long-chain alkanes, high-yield aromatics, low-yield aromatics,
103 and benzene. The seven precursors form twelve semi-volatile products and seven nonvolatile
104 products. The calculations consider dynamic gas-particle conversion of the semi-volatile and
105 nonvolatile products. A more detailed description of the SOA module and parameters used in
106 gas-to-particle transfer calculation is provided in the part I paper (Hu et al., 2015) and references
107 therein.

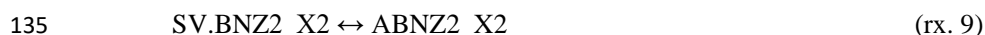
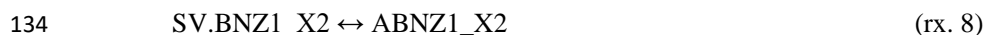
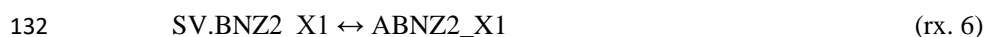
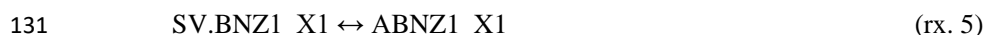
108 The original SOA module described above was modified to have the source
109 apportionment capability inherent in the UCD/CIT model. SOA source apportionment is
110 predicted by tracking the SOA precursor emissions from different sources individually through
111 all atmospheric processes as they react to form low-volatility products that can partition to the
112 particle phase based on the SOA module described above. This approach was initially developed
113 for source apportionment of secondary inorganic aerosols, such as nitrate, sulfate, and
114 ammonium (Mysliwiec and Kleeman, 2002; Ying and Kleeman, 2006). Later, this approach was
115 applied for SOA source apportionment in California using the Caltech Atmospheric Chemistry
116 Mechanism (Chen et al., 2010; Kleeman et al., 2007) and in Texas using the SAPRC99
117 mechanism (Zhang and Ying, 2011; Zhang and Ying, 2012). In the current study, the SAPRC11
118 mechanism was used and expanded to track the reactions of SOA precursors emitted from
119 different sources. Chemical reaction products leading to SOA formation are labeled with the



120 source-identity of the reactant so that source attribution information is preserved. For the
 121 example of benzene (BENZ) reaction with OH forming benzene derived SOA,



125 where SV.BNZ1 and SV.BNZ2 represents the two semi-volatile products that partition between
 126 gas and particle phase, and ABNZ1 and ABNZ2 represent the particle phase SOA products from
 127 SV.BNZ1 and SV.BNZ2, respectively. If there are two sources for BENZ, then BENZ is
 128 expanded into two species BENZ_X1 and BENZ_X2 in the model. The above pathways (rx1 –
 129 rx3) are then expanded as:



136 Thus, the SOA products from BENZ ABNZ1_X1, ABNZ1_X2, ABNZ2_X1 and
 137 ABNZ2_X2 contain the information needed to calculate source contributions to the SOA
 138 concentrations.

139 **2.2 Model Application**

140 The UCD/CIT model was applied to simulate the concentrations and sources of POA and
 141 SOA during ~ a decadal period (9 years from 2000 January 1st to 2008 December 31st) over



142 California using a one-way nesting technique added to the UCD/CIT model (Zhang and Ying,
143 2010). The parent domain covers the entire state of California using a 24km horizontal grid
144 resolution and two nested domains cover the most populated areas (> 92% of California total
145 population) using a 4km horizontal grid resolution. Emissions of the seven SOA precursors were
146 grouped into nine source categories: on-road gasoline engines, off-road gasoline engines, on-
147 road diesel engines, off-road diesel engines, wood smoke, meat cooking, high sulfur fuel
148 combustion, other anthropogenic sources (including solvent usage, waste disposal emissions etc.),
149 and the biogenic sources. Primary PM emissions were also grouped into these 9 source
150 categories. Particulate composition, number and mass concentrations in the range between 0.01
151 and 10 μm in diameter were represented in 15 size bins with the first 5 bins for $\text{PM}_{0.1}$ (0.01 to 0.1
152 μm) in the model. Biogenic emissions were generated using the U.S. EPA's biogenic emission
153 inventory system (BEIS3.14). The Weather Research and Forecasting model (WRF) v3.1.1
154 (William C. Skamarock, June 2008) was used to simulate the 24 km and 4 km hourly
155 meteorology fields (wind, temperature, humidity, precipitation, radiation, air density, and mixing
156 layer height) that drove the UCD/CIT model simulations. WRF simulations were initialized and
157 bounded by the North American Regional Reanalysis (NARR) data with 32 km resolution and 3-
158 hour time resolution. The four-dimensional data assimilation (FDDA) (Liu et al., 2005)
159 technique was used and the surface friction velocity (u^*) in the WRF model was increased by 50%
160 to improve the surface wind predictions as suggested by previous studies (Hu et al., 2012; Hu et
161 al., 2010; Mass, 2010). Details of the modeling domains, vertical cell spacing, preparation of
162 emissions and meteorological inputs are provided in the first paper in the series (Hu et al., 2015).



163 3. Results

164 3.1 Concentrations of POA and SOA

165 Hourly POA and SOA concentrations in multiple size fractions were calculated
166 throughout the 9-year simulation period, and then averaged to daily and monthly average
167 concentrations. Although the focus of the current study is $PM_{0.1}$ POA and SOA, the predicted
168 $PM_{2.5}$ OA concentrations were also calculated and compared to measurements as a confidence
169 building exercise (since $PM_{0.1}$ measurements are not routinely available). Model calculations
170 predict organic matter (OM) concentrations while ambient measurements quantify organic
171 carbon (OC) concentrations. Simulated OM concentrations are converted to OC concentrations
172 using an OM/OC ratio of 1.6 for POA (Turpin and Lim, 2010) and species-specific OM/OC
173 ratios for SOA species taken from Table 1 in Carlton et al. (2010). Detailed evaluation of the
174 model performance for $PM_{2.5}$ OC (and other PM / gaseous species) has been presented in the first
175 paper in the series (Hu et al., 2015). In summary, predicted monthly average $PM_{2.5}$ OC has a
176 mean fractional bias of -0.32 and a mean fractional error of 0.43. Monthly mean fractional bias
177 (MFB) and mean fractional errors (MFE) calculated using daily average OC generally meet the
178 model performance criteria proposed by Boylan and Russell (2006).

179 Figure 1 illustrates the time series of the predicted and measured monthly-average total
180 $PM_{2.5}$ OC concentrations at six major urban locations (a) Sacramento, (b) San Jose, (c) Fresno, (d)
181 Bakersfield, (e) Los Angeles, and (f) Riverside. Measured $PM_{2.5}$ OC concentrations at all sites
182 show strong seasonal variation with higher concentrations in winter months and lower
183 concentrations in summer months. OC concentrations predicted by the UCD/CIT model
184 generally capture the monthly average concentrations and seasonal variations with MFB ranging



185 from -0.31 to 0.19 and MFE ranging from 0.4 to 0.59. However, the model predicts much weaker
186 trends of PM_{2.5} OC over the 9 years at Los Angeles and Riverside, indicating that the declining
187 emission trends might not be well represented in the inventory. At Sacramento and Fresno, the
188 measured monthly average OC concentrations frequently exceeded 10 µg/m³ in winter and the
189 maximum monthly OC concentrations reached or exceeded ~25 µg/m³. Wood smoke is predicted
190 to be the dominant OC source at the two locations, contributing over 70% of the total OC
191 concentrations on average. Wood smoke is also predicted to be the dominant OC source in
192 winter at San Jose and Bakersfield. Model calculations tend to over-predict the winter OC
193 concentrations at San Jose, indicating the wood smoke emissions are likely over-estimated in this
194 area. Model calculations generally under-predict OC in summer when concentrations are lower.
195 Meat cooking and other anthropogenic sources are predicted to be the largest sources in summer
196 at Sacramento, San Jose, Fresno, and Bakersfield. Together these two categories contribute over
197 86% of the total predicted OC in summer. Both measured and predicted seasonal variation is
198 weaker at Los Angeles and Riverside than in Northern California due to smaller wood smoke
199 contributions. Meat cooking and other anthropogenic sources make the largest predicted
200 contributions to OA at these two Southern California locations. Mobile sources (gasoline and
201 diesel engines) also contribute approximately 30% of the total PM_{2.5} OC at Los Angeles. Model
202 calculations tend to under-predict PM_{2.5} OC concentrations in all seasons in 2000-2006 at
203 Riverside (approximately 80 km downwind of the Los Angeles urban center). Intense emissions
204 transported from the upwind Los Angeles areas along with the meteorology and topography
205 enhances photo-oxidation of volatile organic compounds (VOCs) and formation of SOA at this
206 location. A measurement study of organic aerosols at Riverside in summer indicated high SOA
207 fraction of the total OA with an average SOA/OA ratio of 0.74 (Docherty et al., 2008). The



PM_{2.5} OC under-prediction at Riverside during summer and the general under-prediction in summer at other sites may indicate that some important precursors and pathways of PM_{2.5} SOA are missing or only partially included in the current SOA module, such as SOA formation from glyoxal and methylglyoxal (Ervens and Volkamer, 2010; Fu et al., 2008; Ying et al., 2015) and from aerosol aqueous phase chemistry (Volkamer et al., 2009), the conversion of intermediate volatility compounds to SOA (Jathar et al., 2014; Zhao et al., 2014), or SOA forming with higher yields than included in the module (Zhang et al., 2014; Cappa et al., 2016).

Figure 2a compares the average PM_{2.5} OC/mass ratios estimated from ambient measurements and the values predicted by the UCD/CIT model over the 9-year study period at seven representative urban locations. At each site, daily average measured concentrations of the PM_{2.5} total mass and OC were obtained from California Air Resources Board (CARB) (CARB, 2011) “1 in 3” sampling network and averaged over the 9 year period. Predicted concentrations on the corresponding days were extracted and averaged for the comparison. The average OC/mass ratios were then calculated. The observed average OC/mass ratios vary in the range of 0.24 (at Riverside) to 0.45 (at Sacramento). The predicted average OC/mass ratios are in relatively good agreement with measured values at Los Angeles, Riverside, and Bakersfield (difference < 20%), but not at Sacramento, San Jose, Fresno, and El Cajon (difference > 35%). The predicted average OC/mass ratios are consistently lower than observed ratios, by 0.01 (3% at Los Angeles) to 0.22 (48% at Sacramento). This under-prediction is partly attributed to the under-prediction of OC concentrations, especially the SOA concentrations, but also to the over-prediction of total mass concentrations due to over-estimated dust emissions (Hu et al., 2014a; Hu et al., 2015). A sensitivity analysis was conducted by removing the dust concentrations from the predicted PM_{2.5} mass (Figure 2a). The average predicted OC/mass ratio increased from 0.22



231 to 0.29 (average across the seven sites), compared to the observed ratio of 0.33. Omission of dust
232 from the model predictions improves agreement with OC/mass measurements at all sites except
233 central Los Angeles, although OC/mass without dust is still lower than measurements at four
234 sites (Sacramento, San Jose, Fresno, and El Cajon) indicating OC predictions are likely biased
235 low at these locations.

236 Figure 2b compares the predicted and observed OC/mass ratios in the ultrafine ($PM_{0.1}$) or
237 quasi-ultrafine ($PM_{0.18}$, $PM_{0.25}$) particles. The ultrafine/quasi-ultrafine measurement data were
238 compiled in a previous study (Hu et al., 2014a) from published literature (Herner et al., 2005;
239 Kim et al., 2002; Krudysz et al., 2008; Sardar et al., 2005a; Sardar et al., 2005b). The ultrafine or
240 quasi-ultrafine data are more sparse than the $PM_{2.5}$ data, but still cover a sufficient total number
241 of days to allow for robust comparison. The observed OC/mass ratios in ultrafine/quasi-ultrafine
242 sizes vary from 0.43 (at Modesto) to 0.71 (at USC). The predicted ultrafine/quasi-ultrafine
243 OC/mass ratios generally agree well with observed values at all sites. The generally better
244 agreement of OC/mass ratios in the ultrafine/quasi-ultrafine size range compared to the $PM_{2.5}$
245 size range reflects the fact that SOA formation and dust emissions make limited contributions to
246 ultrafine/quasi-ultrafine concentrations. Condensation of SOA mostly takes place in the particle
247 accumulation mode, and is generally not dominant in the ultrafine size range due to the increase
248 in the saturation vapor pressure above small particles (Kelvin effect). Dust components mainly
249 contribute to coarse and fine particles, but make little contribution to the ultrafine particles.

250 The primary and secondary fraction of total OA cannot be directly measured in ambient
251 OA samples. A few indirect methods have been developed to estimate the POA and SOA
252 concentrations, such as molecular marker-based method (Daher et al., 2011; Daher et al., 2012;
253 Ham and Kleeman, 2011; Kleindienst et al., 2007), elemental carbon (EC) tracer method



(Cabada et al., 2004; Lim et al., 2003; Polidori et al., 2007; Polidori et al., 2006; Turpin and Huntzicker, 1995), water soluble organic carbon content method (Weber et al., 2007), aerosol mass spectrometry factorization method (Aiken et al., 2008; Lanz et al., 2007; Ulbrich et al., 2009), and the un-explained fraction of OA by tracers for major POA categories (Chen et al., 2010; Schauer and Cass, 2000). In the current study, $\text{PM}_{2.5}$ SOA concentrations were estimated by the molecular marker Chemical Mass Balance (CMB) method (Daher et al., 2012) during sampling periods in 2005-2007 at four locations. $\text{PM}_{2.5}$ POA concentrations were then estimated by subtracting $\text{PM}_{2.5}$ SOA concentrations estimated by the CMB method from the total measured OA concentrations. Figure 3 shows the $\text{PM}_{2.5}$ POA and SOA concentrations predicted by the UCD/CIT model (right dark columns) compared to the $\text{PM}_{2.5}$ POA and SOA concentrations estimated using the CMB method (left gray columns). Error bars represent the standard deviation of concentrations estimated during the sampling periods. The total $\text{PM}_{2.5}$ OA (i.e., POA + SOA) concentrations predicted by the UCD/CIT model generally agree with measured values (with fractional bias within $\pm 35\%$) except at the Riverside site (with a fraction bias of -63%). But the $\text{PM}_{2.5}$ SOA concentrations predicted by the UCD/CIT model appear to be a factor of 2~3 lower than the SOA concentrations estimated by the CMB method (ratio ranging from 2.2 at Riverside to 2.8 at WSanG). The $\text{PM}_{2.5}$ POA concentrations predicted by the UCD/CIT model are higher than those estimated by the CMB method at WSanG and ESanG1. This may reflect the effects of POA volatility. Studies have indicated that some fraction of POA emissions will evaporate, and this material may undergo photo-oxidation and condense back to particle phase (Robinson et al., 2007). In the current model, POA is treated as non-volatile. Thus, no such evaporation occurs. However, the substantial under-prediction of $\text{PM}_{2.5}$ SOA at all sites suggests that some SOA precursors and pathways are likely missing from the current SOA mechanism. Both $\text{PM}_{2.5}$ POA



277 and SOA are under-predicted at Riverside, indicating that some important sources are likely
278 missing in that area.

279 Figure 4 illustrates the predicted total $\text{PM}_{0.1}$ OA concentrations (Figure 4a) and the
280 predicted ratios of SOA to total OA averaged over the 9 year modeling period (Figure 4b). High
281 total $\text{PM}_{0.1}$ OA concentrations with maximum concentrations $> 2 \mu\text{g}/\text{m}^3$ are located in urban
282 areas where the POA emissions are large due to human activities. Predicted $\text{PM}_{0.1}$ SOA generally
283 accounts for less than 10% of total $\text{PM}_{2.5}$ OA at urban areas, but predicted SOA contribute to
284 10~20% of total OA in suburban areas, and contribute to 20~50% in rural areas. The spatial
285 distribution of $\text{PM}_{2.5}$ SOA concentrations and the SOA to total OA ratios (shown in Figure S1)
286 are generally similar to those of $\text{PM}_{0.1}$, but $\text{PM}_{0.1}$ OA has sharper spatial gradients and the $\text{PM}_{0.1}$
287 SOA fraction is lower than $\text{PM}_{2.5}$, indicating POA contributes more in the ultrafine size range.

288 Figure 5 shows the contributions from the 9 precursor species to the $\text{PM}_{0.1}$ SOA
289 concentrations (results of $\text{PM}_{2.5}$ SOA are shown in Figure S2). Maximum SOA concentrations
290 are located in southern part of the SJV. Monoterpenes, sesquiterpenes, oligomers, and long
291 alkanes are the most important precursors, contributing over 90% of the total SOA in most areas,
292 while other precursors (xylene, toluene, and benzene) in total contribute less than $10 \text{ ng}/\text{m}^3$ to
293 SOA concentrations. These finding are very dependent on the treatment of vapor wall losses
294 during the formulation of the SOA model. The contributions from different precursors to SOA
295 concentrations have very different spatial distributions. Long chain alkanes form SOA mainly in
296 the urban areas of Southern California and in the middle-southern portion of the SJV. Isoprene,
297 monoterpenes, and sesquiterpenes form SOA at coastal and foothill locations where the biogenic
298 emissions are greatest. The longer lifetime of long chain alkanes than isoprene leads to a broader
299 spatial distribution for the SOA derived from alkanes. The spatial distribution of oligomers of



anthropogenic SOA (Oligomer_A) and biogenic SOA (Oligomer_B) reflects the patterns of SOA derived from long chain alkanes and the total biogenic species. The relative spatial patterns associated with each precursor are generally not sensitive to the exact formulation of the SOA model (see section 3.3).

3.2 Sources of POA and SOA

Figure 6 displays the time series of monthly average $PM_{0.1}$ SOA source contributions at the six major urban locations. $PM_{0.1}$ SOA concentrations are high in summer ($100\sim300\text{ ng/m}^3$) and low ($20\sim50\text{ ng/m}^3$) in winter, reflecting the seasonal variation in photochemistry. $PM_{0.1}$ SOA concentrations are higher at Fresno and Bakersfield than other sites due to larger biogenic source contributions. Biogenic emissions are the largest source of $PM_{0.1}$ SOA across all sites, followed by the other anthropogenic sources (mainly solvent usage and waste disposal emissions, see Figure S5). On-road gasoline engines are an important source of SOA at Los Angeles and Riverside. Similar source contributions to $PM_{2.5}$ SOA are found and shown in Figure S3 in the Supplemental Materials.

Figure 7 shows the predicted regional source contributions of $PM_{0.1}$ POA averaged over the 9 year modeling period. The dominant regional sources of $PM_{0.1}$ POA are predicted to be wood smoke, meat cooking, other anthropogenic sources, on-road gasoline and off-road diesel. Wood smoke is the dominant POA source especially in Northern California, with the maximum $PM_{0.1}$ POA contribution exceeding $1\text{ }\mu\text{g/m}^3$. Meat cooking and mobile (on-road and off-road) sources are the major sources in urban areas, especially in metropolitan areas such as Greater Los Angeles Area and the San Francisco Bay Area. Other anthropogenic sources is another major category in the urban centers in the SJV and also the Los Angeles areas. High sulfur content fuel



sources are mainly located around the ports in the Los Angeles and San Francisco Bay areas. The regional source contributions of $PM_{0.1}$ POA are quite different from those of $PM_{2.5}$ POA (shown in Figure S4). The $PM_{2.5}$ POA source contributions are much more widespread than the $PM_{0.1}$ POA sources contributions because $PM_{2.5}$ has a longer lifetime due to slower deposition and coagulation compared to $PM_{0.1}$. For example, the mobile sources and the other anthropogenic sources contribute greatly to $PM_{2.5}$ POA throughout the entire SJV, but only contribute to $PM_{0.1}$ POA in urban centers.

Figure 8 shows the predicted regional source contributions of $PM_{0.1}$ SOA averaged over the 9 year modeling period (and Figure S6 shows the $PM_{2.5}$ SOA results). Biogenic emission is predicted to be the single largest $PM_{0.1}$ SOA source in the present study. The maximum biogenic $PM_{0.1}$ SOA concentration is up to $0.1 \mu\text{g}/\text{m}^3$ around Bakersfield in the southern SJV. Other anthropogenic sources, on-road gasoline engines, and off-road gasoline engines are predicted to be the dominant anthropogenic sources of $PM_{0.1}$ SOA in California. The spatial distribution of $PM_{0.1}$ SOA concentrations from these anthropogenic sources are similar (but different from the spatial distribution of SOA from biogenic sources) with high concentrations in Southern California. $PM_{0.1}$ SOA formation from on-road diesel engines, off-road diesel engines, wood smoke, meat cooking and high sulfur fuel combustion are small, with $PM_{0.1}$ SOA contributions generally less than a few ng/m^3 . A recent epidemiological study has revealed that anthropogenic $PM_{0.1}$ SOA is highly associated with ischemic heart disease mortality (Ostro et al., 2015). Therefore, the results in this study suggest that control of solvent usage, waste disposal, and mobile emissions should be considered to protect public health in California, but the exact determination of source controls will need to be evaluated after the SOA formation mechanism is updated.



3.3 Influence of vapor wall losses on SOA exposure in California

The SOA concentrations predicted in the current study are based on the SOA yield data measured in chamber experiments. A recent study has demonstrated that organic vapors can be lost to chamber walls during SOA formation experiments resulting in SOA yields that are biased low (Zhang et al., 2014). Efforts have been carried out to parameterize the effect of vapor wall losses on SOA formation in the UCD/CIT air quality model to account for this effect when predicting ambient SOA concentrations in Southern California (Cappa et al., 2015). SOA concentrations are predicted to increase by factors of 2-5 with low vapor wall loss rates, and by factors of 5-10 with high vapor wall loss rates, compared to the concentrations in the simulations with no consideration of vapor wall losses. Here we further analyzed the changes in the population weighted concentrations (PWCs) of SOA when vapor wall losses are accounted for. Two sets of simulations (scenarios) conducted by Cappa et al (2015) are considered, one with the low-NO_x, high-yield parameters (denoted as “highyield”) and the other with high-NO_x, low-yield parameters (denoted as “lowyield”). Each set of simulations included three vapor wall loss cases, i.e., no consideration of vapor wall losses (denoted as “base”), low vapor wall loss rates (denoted as “lowwallloss”), and high vapor wall loss rates (denoted as “highwallloss”). PWCs of SOA are calculated for six counties in the Southern California for the six scenarios, respectively. Spatial difference in exposure is important in cohort studies, therefore the relative changes of PWCs among counties are examined. Figure 9 shows the PWCs of SOA and their relative changes in different scenarios in the six counties. The results indicate that PWCs of SOA increase substantially by accounting for vapor wall losses in all counties (panel a). However, the spatial pattern of SOA PWC, as characterized by normalizing the PWC for each location by the PWC in Orange County, is very similar in all scenarios (panel b). Consequently, accounting for vapor



368 wall losses changes the SOA exposure ratio in different counties by only a small extent of < 15%
369 for most scenarios/counties (panel c). These results suggest that future simulations that account
370 for vapor wall losses in SOA simulations will yield increased absolute values of concentrations
371 but will have spatial patterns that are similar to the basecase results in the current paper when
372 used for epidemiology studies.

373 Figure 9 suggests that associations between anthropogenic SOA and health effects identified in
374 previous epidemiological studies will prove robust to future updates in SOA models. This
375 finding also extends to the spatial pattern of individual SOA precursors. The influence of vapor
376 wall losses on exposure to SOA formed from different precursors (i.e., long alkanes, aromatics,
377 isoprene, sesquiterpenes, and monoterpenes) is shown in Figures S7-S11. In all cases, the spatial
378 pattern of PWC for SOA derived from each precursor is similar under all treatments of wall
379 losses. Long alkanes and aromatics are mainly from anthropogenic sources, and isoprene,
380 sesquiterpenes, and monoterpenes are mostly from biogenic sources. Further detailed
381 interpretation of source contributions to SOA and associated health effects should only be carried
382 out after new exposure fields are calculated using the latest SOA models.

383 **4. Conclusions**

384 The source-oriented UCD/CIT model was applied to predict the concentrations and
385 sources of $PM_{0.1}$ POA and SOA in California for a 9 year (2000 - 2008) modeling period with 4
386 km horizontal resolution to provide data for health effects studies. As a confidence building
387 measure, predicted total $PM_{2.5}$ OC concentrations (primary + secondary) and the $PM_{2.5}$ and $PM_{0.1}$
388 OC/mass ratios generally agree with measured values at fixed point locations. Compared to the
389 POA and SOA concentrations estimated from measurements at 4 sites using the CMB method,



the $\text{PM}_{2.5}$ total OA concentrations predicted by the UCD/CIT model have a fractional bias within $\pm 35\%$ except at the Riverside site. The CMB model estimated $\text{PM}_{2.5}$ SOA concentrations accounted for 13–37% of total OA while the UCD/CIT SOA concentrations accounted for 4–11% of total OA. POA volatility, incomplete SOA formation mechanism, and/or missing sources may account for the discrepancy. For these reasons, the current study focuses on the $\text{PM}_{0.1}$ size fraction.

$\text{PM}_{0.1}$ OA has larger contributions from primary sources than the $\text{PM}_{2.5}$ size fraction. Wood smoke is found to be the single biggest source of $\text{PM}_{0.1}$ OA in winter in California, and meat cooking, mobile sources and other anthropogenic sources (mainly solvent usage, and waste disposal) are the most important sources in summer, but these rankings are sensitive to the SOA model used in the calculation. Biogenic emissions are predicted to be the largest $\text{PM}_{0.1}$ SOA source, followed by the other anthropogenic sources, and mobile sources. A recent epidemiological study has revealed that anthropogenic $\text{PM}_{0.1}$ SOA is highly associated with ischemic heart disease mortality (Ostro et al., 2015). Therefore, the results in the present study suggest that control of solvent usage, waste disposal, and mobile emissions should be considered to protect public health in California, but detailed source control programs can only be carried out after revised calculations are performed using updated SOA models. The predicted spatial distributions of the concentrations and sources of POA and SOA in $\text{PM}_{0.1}$ over the 9-year periods provide detailed information for epidemiological studies to further investigate the associations with other health outcomes, and these spatial patterns are generally not sensitive to the treatment of wall losses in the SOA model formulation. All model results included in the current manuscript can be downloaded free of charge at <http://faculty.engineering.ucdavis.edu/kleeman/>.



412 **Acknowledgement**

413 This study was funded by the United States Environmental Protection Agency under Grant No.
414 R83386401. Although the research described in the article has been funded by the United States
415 Environmental Protection Agency it has not been subject to the Agency's required peer and
416 policy review and therefore does not necessarily reflect the reviews of the Agency and no official
417 endorsement should be inferred.

418

419 **References**

- 420 Aiken, A.C. et al., 2008. O/C and OM/OC Ratios of Primary, Secondary, and
421 Ambient Organic Aerosols with High-Resolution Time-of-Flight Aerosol
422 Mass Spectrometry. *Environ Sci Technol*, 42(12): 4478-4485.
- 423 Boylan, J.W. and Russell, A.G., 2006. PM and light extinction model
424 performance metrics, goals, and criteria for three-dimensional air
425 quality models. *Atmos Environ*, 40(26): 4946-4959.
- 426 Cabada, J.C. et al., 2004. Estimating the secondary organic aerosol contribution
427 to PM_{2.5} using the EC tracer method. *Aerosol Science and Technology*,
428 38: 140-155.
- 429 Cao, J.J., Xu, H.M., Xu, Q., Chen, B.H. and Kan, H.D., 2012. Fine Particulate Matter
430 Constituents and Cardiopulmonary Mortality in a Heavily Polluted
431 Chinese City. *Environ Health Persp*, 120(3): 373-378.
- 432 Cappa, C.D. et al., 2015. Simulating secondary organic aerosol in a regional air
433 quality model using the statistical oxidation model – Part 2: Assessing
434 the influence of vapor wall losses. *Atmospheric Chemistry and Physics*
435 *Discussion*, 15: 30081030126.
- 436 CARB, 2011. Database: California Air Quality Data - Selected Data Available for
437 Download <<http://www.arb.ca.gov/aqd/aqcd/aqcdcdld.htm>>.
438 Accessed in 2011.
- 439 Carlton, A.G. et al., 2010. Model Representation of Secondary Organic Aerosol
440 in CMAQv4.7. *Environ Sci Technol*, 44(22): 8553-8560.
- 441 Chen, J.J., Ying, Q. and Kleeman, M.J., 2010. Source apportionment of
442 wintertime secondary organic aerosol during the California regional
443 PM(10)/PM(2.5) air quality study. *Atmos Environ*, 44(10): 1331-1340.



- 444 Daher, N. et al., 2011. Chemical Characterization and Source Apportionment of
445 Fine and Coarse Particulate Matter Inside the Refectory of Santa Maria
446 Delle Grazie Church, Home of Leonardo Da Vinci's "Last Supper".
447 Environ Sci Technol, 45(24): 10344-10353.
- 448 Daher, N. et al., 2012. Characterization, sources and redox activity of fine and
449 coarse particulate matter in Milan, Italy. Atmos Environ, 49(0): 130-141.
- 450 Docherty, K.S. et al., 2008. Apportionment of Primary and Secondary Organic
451 Aerosols in Southern California during the 2005 Study of Organic
452 Aerosols in Riverside (SOAR-1). Environ Sci Technol, 42(20): 7655-
453 7662.
- 454 Dockery, D.W., 2001. Epidemiologic evidence of cardiovascular effects of
455 particulate air pollution. Environ Health Persp, 109: 483-486.
- 456 Dockery, D.W. and Pope, C.A., 1994. Acute Respiratory Effects of Particulate
457 Air-Pollution. Annual Review of Public Health, 15: 107-132.
- 458 Dockery, D.W. et al., 1993. An Association between Air-Pollution and Mortality
459 in 6 United-States Cities. New Engl J Med, 329(24): 1753-1759.
- 460 Ervens, B. and Volkamer, R., 2010. Glyoxal processing by aerosol multiphase
461 chemistry: towards a kinetic modeling framework of secondary organic
462 aerosol formation in aqueous particles. Atmos Chem Phys, 10(17):
463 8219-8244.
- 464 Franklin, M., Zeka, A. and Schwartz, J., 2007. Association between PM_{2.5} and
465 all-cause and specific-cause mortality in 27 US communities. Journal of
466 Exposure Science and Environmental Epidemiology, 17(3): 279-287.
- 467 Fu, T.M. et al., 2008. Global budgets of atmospheric glyoxal and methylglyoxal,
468 and implications for formation of secondary organic aerosols. J Geophys
469 Res-Atmos, 113(D15).
- 470 Ham, W.A. and Kleeman, M.J., 2011. Size-resolved source apportionment of
471 carbonaceous particulate matter in urban and rural sites in central
472 California. Atmos Environ, 45(24): 3988-3995.
- 473 Herner, J.D., Aw, J., Gao, O., Chang, D.P. and Kleeman, M.J., 2005. Size and
474 composition distribution of airborne particulate matter in northern
475 California: I-particulate mass, carbon, and water-soluble ions. J Air
476 Waste Manage, 55(1): 30-51.
- 477 Hu, J., Howard, C.J., Mitloehner, F., Green, P.G. and Kleeman, M.J., 2012. Mobile
478 Source and Livestock Feed Contributions to Regional Ozone Formation
479 in Central California. Environ Sci Technol, 46(5): 2781-2789.
- 480 Hu, J. et al., 2010. Particulate air quality model predictions using prognostic vs.
481 diagnostic meteorology in central California. Atmos Environ, 44(2): 215-
482 226.



- 483 Hu, J. et al., 2014a. Predicting Primary PM_{2.5} and PM_{0.1} Trace Composition
 484 for Epidemiological Studies in California. *Environ Sci Technol*, 48(9):
 485 4971-4979.
- 486 Hu, J. et al., 2014b. Identifying PM_{2.5} and PM_{0.1} Sources for Epidemiological
 487 Studies in California. *Environ Sci Technol*, 48(9): 4980-4990.
- 488 Hu, J. et al., 2015. Long-term particulate matter modeling for health effect
 489 studies in California - Part I: model performance on temporal and
 490 spatial variations. *Atmos Chem Phys*, 15: 3445-3461.
- 491 Jathar, S.H. et al., 2014. Unspeciated organic emissions from combustion
 492 sources and their influence on the secondary organic aerosol budget in
 493 the United States. *P Natl Acad Sci USA*, 111(29): 10473-10478.
- 494 Jathar, S.H. et al., 2016. Water uptake by organic aerosol and its influence on
 495 gas/particle partitioning of secondary organic aerosol in the United
 496 States. *Atmos Environ*, 129: 142-154.
- 497 Kim, S., Shen, S., Sioutas, C., Zhu, Y.F. and Hinds, W.C., 2002. Size distribution
 498 and diurnal and seasonal trends of ultrafine particles in source and
 499 receptor sites of the Los Angeles basin. *J Air Waste Manage*, 52(3): 297-
 500 307.
- 501 Kleeman, M.J. et al., 2009. Source Apportionment of Fine (PM_{1.8}) and Ultrafine
 502 (PM_{0.1}) Airborne Particulate Matter during a Severe Winter Pollution
 503 Episode. *Environ Sci Technol*, 43(2): 272-279.
- 504 Kleeman, M.J. et al., 2007. Source apportionment of secondary organic aerosol
 505 during a severe photochemical smog episode. *Atmos Environ*, 41(3):
 506 576-591.
- 507 Kleindienst, T.E. et al., 2007. Estimates of the contributions of biogenic and
 508 anthropogenic hydrocarbons to secondary organic aerosol at a
 509 southeastern US location. *Atmos Environ*, 41(37): 8288-8300.
- 510 Krall, J.R., Anderson, G.B., Dominici, F., Bell, M.L. and Peng, R.D., 2013. Short-
 511 term Exposure to Particulate Matter Constituents and Mortality in a
 512 National Study of US Urban Communities. *Environ Health Persp*,
 513 121(10): 1148-1153.
- 514 Krudysz, M.A., Froines, J.R., Fine, P.M. and Sioutas, C., 2008. Intra-community
 515 spatial variation of size-fractionated PM mass, OC, EC, and trace
 516 elements in the Long Beach, CA area. *Atmos Environ*, 42(21): 5374-
 517 5389.
- 518 Lanz, V.A. et al., 2007. Source Attribution of Submicron Organic Aerosols
 519 during Wintertime Inversions by Advanced Factor Analysis of Aerosol
 520 Mass Spectra. *Environ Sci Technol*, 42(1): 214-220.



- 521 Laurent, O. et al., 2016a. A Statewide Nested Case-Control Study of Preterm
 522 Birth and Air Pollution by Source and Composition: California, 2001-
 523 2008. Environ Health Persp, <http://dx.doi.org/10.1289/ehp.1510133>.
 524 Laurent, O. et al., 2014. Sources and contents of air pollution affecting term
 525 low birth weight in Los Angeles County, California, 2001-2008. Environ
 526 Res, 134: 488-495.
 527 Laurent, O. et al., 2016b. Low birth weight and air pollution in California:
 528 Which sources and components drive the risk? Environ Int, 92-93: 471-
 529 477.
 530 Le Tertre, A. et al., 2002. Short-term effects of particulate air pollution on
 531 cardiovascular diseases in eight European cities. Journal of
 532 Epidemiology and Community Health, 56(10): 773-779.
 533 Levy, J.I., Diez, D., Dou, Y.P., Barr, C.D. and Dominici, F., 2012. A Meta-Analysis
 534 and Multisite Time-Series Analysis of the Differential Toxicity of Major
 535 Fine Particulate Matter Constituents. American Journal of Epidemiology,
 536 175(11): 1091-1099.
 537 Lim, H.J., Turpin, B.J., Russell, L.M. and Bates, T.S., 2003. Organic and elemental
 538 carbon measurements during ACE-Asia suggest a longer atmospheric
 539 lifetime for elemental carbon. Environ Sci Technol, 37(14): 3055-3061.
 540 Liu, Y., Bourgeois, A., Warner, T., Swerdlin, S. and Hacker, J., 2005. An
 541 implementation of obs-nudging-based FDDA into WRF for supporting
 542 ATEC test operations. 2005 WRF user workshop, Paper 10.7.
 543 Mar, T.F., Norris, G.A., Koenig, J.Q. and Larson, T.V., 2000. Associations
 544 between air pollution and mortality in Phoenix, 1995-1997. Environ
 545 Health Persp, 108(4): 347-353.
 546 Mass, C.F., 2010. University of Washington, Seattle, WA, personal
 547 communication.
 548 Mauderly, J.L. and Chow, J.C., 2008. Health effects of organic aerosols. Inhal
 549 Toxicol, 20(3): 257-288.
 550 Mysliwiec, M.J. and Kleeman, M.J., 2002. Source apportionment of secondary
 551 airborne particulate matter in a polluted atmosphere. Environ Sci
 552 Technol, 36(24): 5376-5384.
 553 Ostro, B., Broadwin, R., Green, S., Feng, W.Y. and Lipsett, M., 2006. Fine
 554 particulate air pollution and mortality in nine California counties:
 555 Results from CALFINE. Environ Health Persp, 114(1): 29-33.
 556 Ostro, B. et al., 2015. Associations of Mortality with Long-Term Exposures to
 557 Fine and Ultrafine Particles, Species and Sources: Results from the
 558 California Teachers Study Cohort. Environ Health Persp,
 559 DOI:10.1289/ehp.1408565.



- 560 Ostro, B. et al., 2010. Long-Term Exposure to Constituents of Fine Particulate
 561 Air Pollution and Mortality: Results from the California Teachers Study.
 562 Environ Health Persp, 118(3): 363-369.
- 563 Pankow, J.F. et al., 2015. Molecular view modeling of atmospheric organic
 564 particulate matter: Incorporating molecular structure and co-
 565 condensation of water. Atmos Environ, 122: 400-408.
- 566 Polidori, A., Arhami, M., Sioutas, C., Delfino, R.J. and Allen, R., 2007.
 567 Indoor/Outdoor Relationships, Trends, and Carbonaceous Content of
 568 Fine Particulate Matter in Retirement Homes of the Los Angeles Basin. J
 569 Air Waste Manage, 57(3): 366-379.
- 570 Polidori, A. et al., 2006. Local and regional secondary organic aerosol: Insights
 571 from a year of semi-continuous carbon measurements at Pittsburgh.
 572 Aerosol Science and Technology, 40(10): 861-872.
- 573 Pope, C.A. et al., 2002. Lung cancer, cardiopulmonary mortality, and long-term
 574 exposure to fine particulate air pollution. Jama-Journal of the American
 575 Medical Association, 287(9): 1132-1141.
- 576 Pope, C.A. and Dockery, D.W., 2006. Health effects of fine particulate air
 577 pollution: Lines that connect. J Air Waste Manage, 56(6): 709-742.
- 578 Robinson, A.L. et al., 2007. Rethinking Organic Aerosols: Semivolatile
 579 Emissions and Photochemical Aging. Science, 315(5816): 1259-1262.
- 580 Sardar, S.B., Fine, P.M., Mayo, P.R. and Sioutas, C., 2005a. Size-fractionated
 581 measurements of ambient ultrafine particle chemical composition in Los
 582 Angeles using the NanoMOUDI. Environ Sci Technol, 39(4): 932-944.
- 583 Sardar, S.B., Fine, P.M. and Sioutas, C., 2005b. Seasonal and spatial variability
 584 of the size-resolved chemical composition of particulate matter (PM₁₀)
 585 in the Los Angeles Basin. J Geophys Res-Atmos, 110(D7).
- 586 Schauer, J.J. and Cass, G.R., 2000. Source apportionment of wintertime gas-
 587 phase and particle-phase air pollutants using organic compounds as
 588 tracers. Environ Sci Technol, 34(9): 1821-1832.
- 589 Seinfeld, J.H. and Pankow, J.F., 2003. Organic atmospheric particulate material.
 590 Annual Review of Physical Chemistry, 54: 121-140.
- 591 Turpin, B.J. and Huntzicker, J.J., 1995. Identification of Secondary Organic
 592 Aerosol Episodes and Quantitation of Primary and Secondary Organic
 593 Aerosol Concentrations during Scaqs. Atmos Environ, 29(23): 3527-
 594 3544.
- 595 Turpin, B.J. and Lim, H.J., 2010. Species contributions to PM_{2.5} mass
 596 concentrations: revisiting common assumptions for estimating organic
 597 mass. Aerosol Science and Technology, 35:1: 602-610.



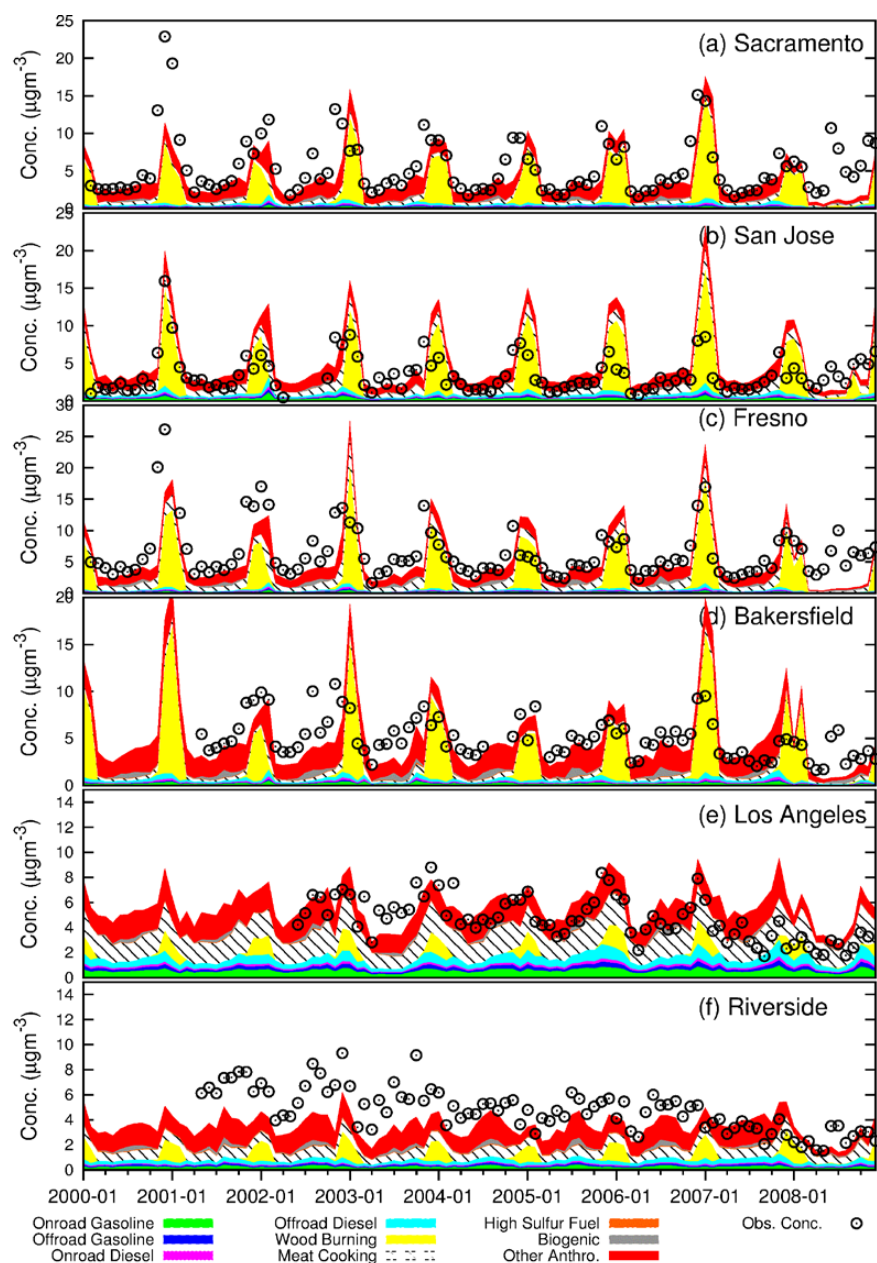
- 598 Ulbrich, I.M., Canagaratna, M.R., Zhang, Q., Worsnop, D.R. and Jimenez, J.L.,
 599 2009. Interpretation of organic components from Positive Matrix
 600 Factorization of aerosol mass spectrometric data. *Atmos Chem Phys*,
 601 9(9): 2891-2918.
- 602 Volkamer, R., Ziemann, P.J. and Molina, M.J., 2009. Secondary Organic Aerosol
 603 Formation from Acetylene (C₂H₂): seed effect on SOA yields due to
 604 organic photochemistry in the aerosol aqueous phase. *Atmos. Chem.*
 605 *Phys.*, 9(6): 1907-1928.
- 606 Weber, R.J. et al., 2007. A study of secondary organic aerosol formation in the
 607 anthropogenic-influenced southeastern United States. *J Geophys Res-*
 608 *Atmos*, 112(D13).
- 609 William C. Skamarock, J.B.K., Jimmy Dudhia, David O Gill, Dale M. Barker,
 610 Michael G. Duda, Xiang-Yu Huang, Wei Wang, and Jordan G. Powers, June
 611 2008. A Description of the Advanced Research WRF Version 3. NCAR
 612 Technical Note NCAR/TN-475+STR.
- 613 Ying, Q. and Kleeman, M.J., 2004. Efficient Source Apportionment of Airborne
 614 Particulate Matter Using an Internally Mixed Air Quality Model with
 615 Artificial Tracers. *Environmental Science and Engineering (China)*, 1(1):
 616 91-99.
- 617 Ying, Q. and Kleeman, M.J., 2006. Source contributions to the regional
 618 distribution of secondary particulate matter in California. *Atmos*
 619 *Environ*, 40(4): 736-752.
- 620 Ying, Q., Li, J. and Kota, S.H., 2015. Significant Contributions of Isoprene to
 621 Summertime Secondary Organic Aerosol in Eastern United States.
 622 *Environ Sci Technol*, 49(13): 7834-7842.
- 623 Ying, Q., Lu, J., Kaduwela, A. and Kleeman, M., 2008. Modeling air quality
 624 during the California Regional PM₁₀/PM_{2.5} Air Quality Study (CPRAQS)
 625 using the UCD/CIT Source Oriented Air Quality Model - Part II. Regional
 626 source apportionment of primary airborne particulate matter. *Atmos*
 627 *Environ*, 42(39): 8967-8978.
- 628 Zhang, H. and Ying, Q., 2011. Secondary organic aerosol formation and source
 629 apportionment in Southeast Texas. *Atmos Environ*, 45(19): 3217-3227.
- 630 Zhang, H. and Ying, Q., 2012. Secondary organic aerosol from polycyclic
 631 aromatic hydrocarbons in Southeast Texas. *Atmos Environ*, 55(0): 279-
 632 287.
- 633 Zhang, H.L. and Ying, Q., 2010. Source apportionment of airborne particulate
 634 matter in Southeast Texas using a source-oriented 3D air quality model.
 635 *Atmos Environ*, 44(29): 3547-3557.



- 636 Zhang, Q. et al., 2007. Ubiquity and dominance of oxygenated species in
637 organic aerosols in anthropogenically-influenced Northern Hemisphere
638 midlatitudes. *Geophysical Research Letters*, 34(13): L13801.
- 639 Zhang, X. et al., 2014. Influence of vapor wall loss in laboratory chambers on
640 yields of secondary organic aerosol. *P Natl Acad Sci USA*, 111(16): 5802-
641 5807.
- 642 Zhao, Y.L. et al., 2014. Intermediate-Volatility Organic Compounds: A Large
643 Source of Secondary Organic Aerosol. *Environ Sci Technol*, 48(23):
644 13743-13750.
- 645

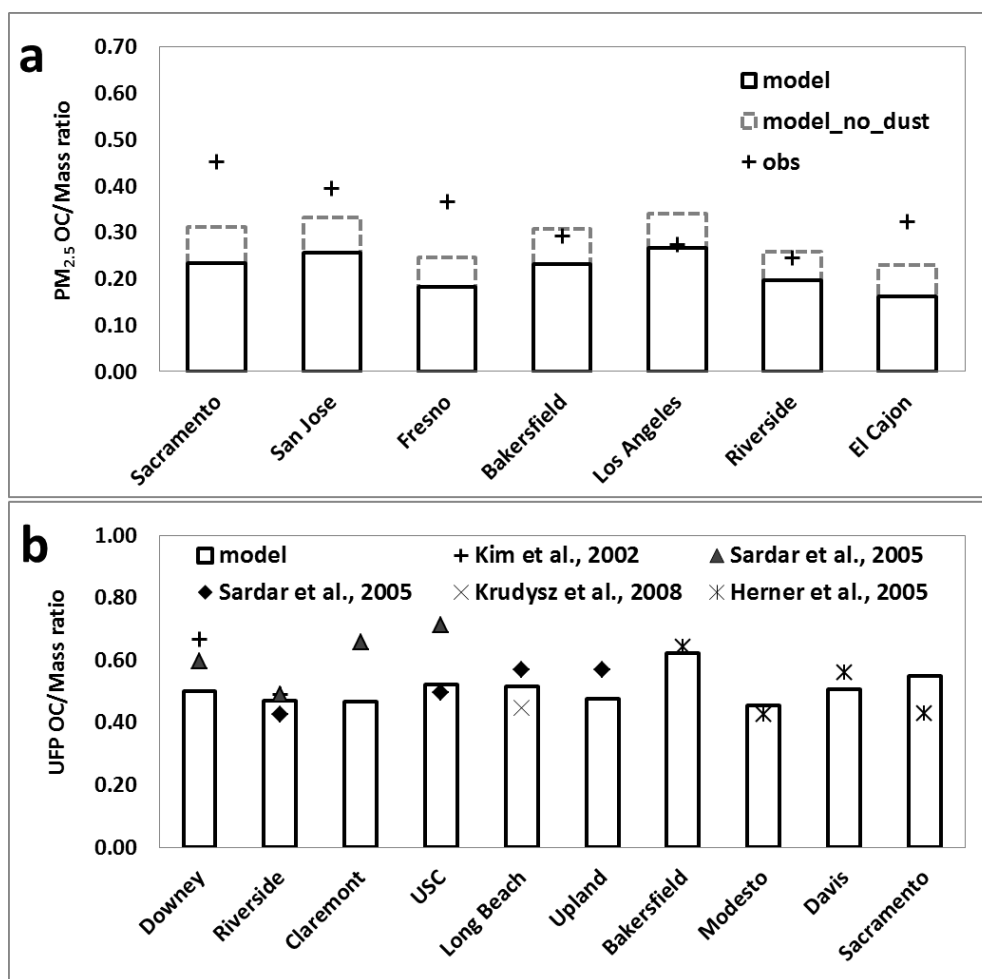


646 Figures and Tables



647

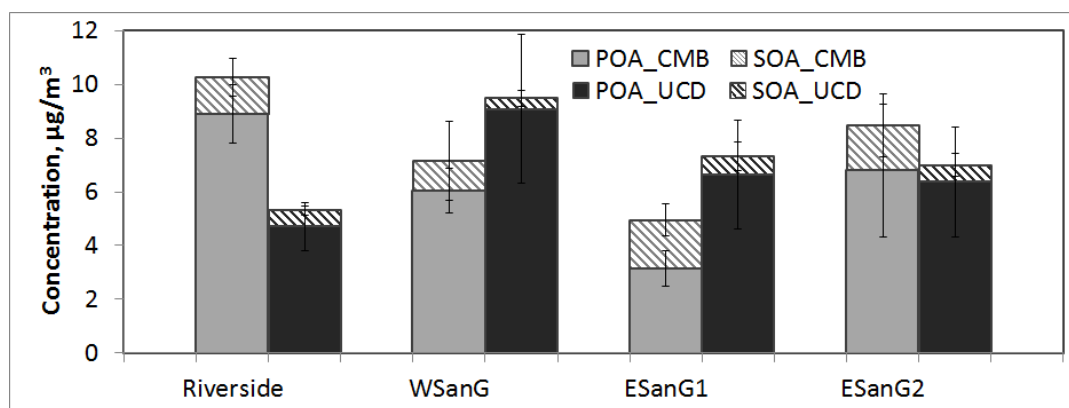
648 Figure 1. Monthly source contributions to $PM_{2.5}$ total OC at 6 urban sites. Observed total OC
 649 concentrations are indicated by the dot-circles, and predicted OC concentrations from different
 650 sources are indicated by the colored areas.



651

652 Figure 2. Observed (obs) and predicted (model) OC/Mass ratios in (a) PM_{2.5} and (b) ultrafine and
 653 quasi-ultrafine PM. In (a), a sensitivity analysis is conducted by removing the dust concentration
 654 from the PM_{2.5} total mass (model_no_dust). The ultrafine and quasi-ultrafine data in (b) are
 655 extracted from published literature as indicated in the figure.

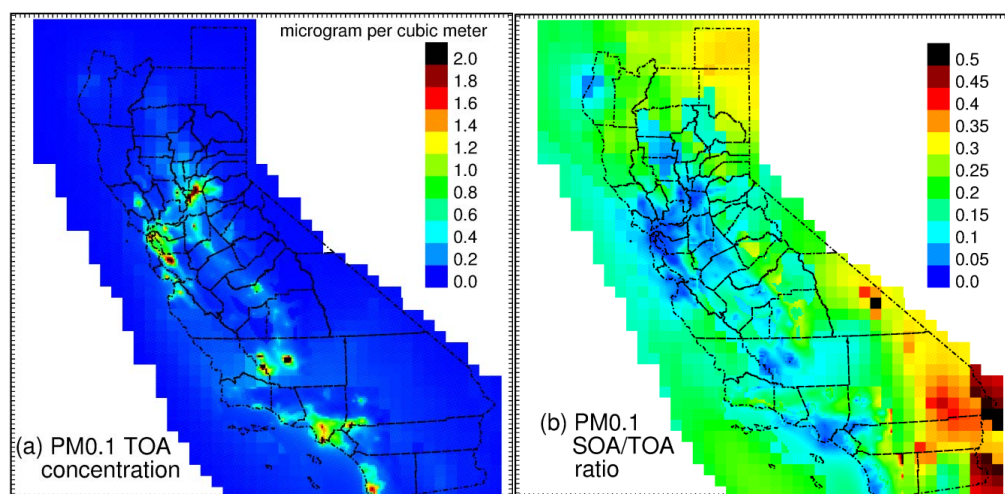
656



657

658 Figure 3. POA and SOA concentrations estimated by the CMB method (left gray columns) and
 659 predicted by the UCD/CIT model (right dark columns). Error bars represent the standard
 660 deviation of concentrations estimated during the sampling periods by both methods. The data are
 661 for sampling periods in 2005-2007 at four sites in Southern California.

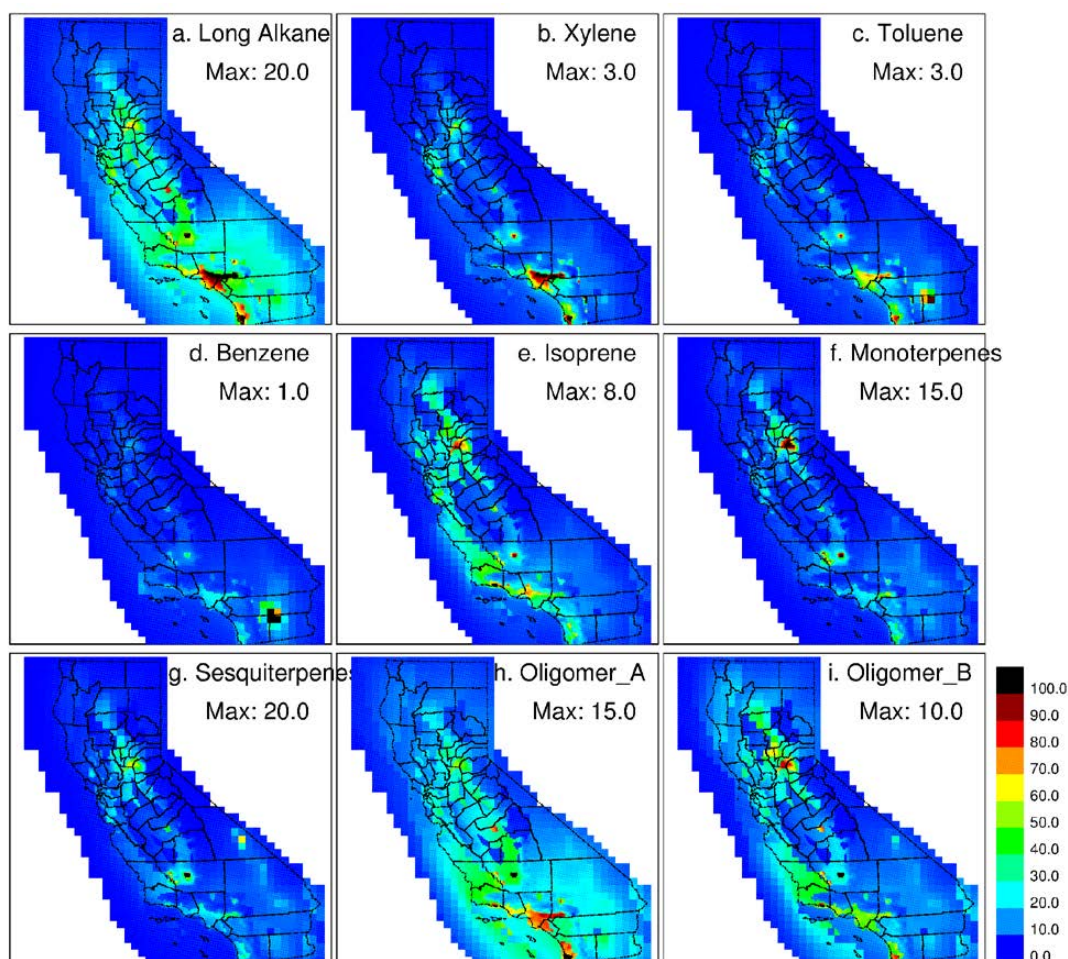
662



663

664 Figure 4. Predicted 9-year average (a) PM_{0.1} Total OA (TOA) concentration and (b) PM_{0.1}
 665 SOA/TOA ratio in California.

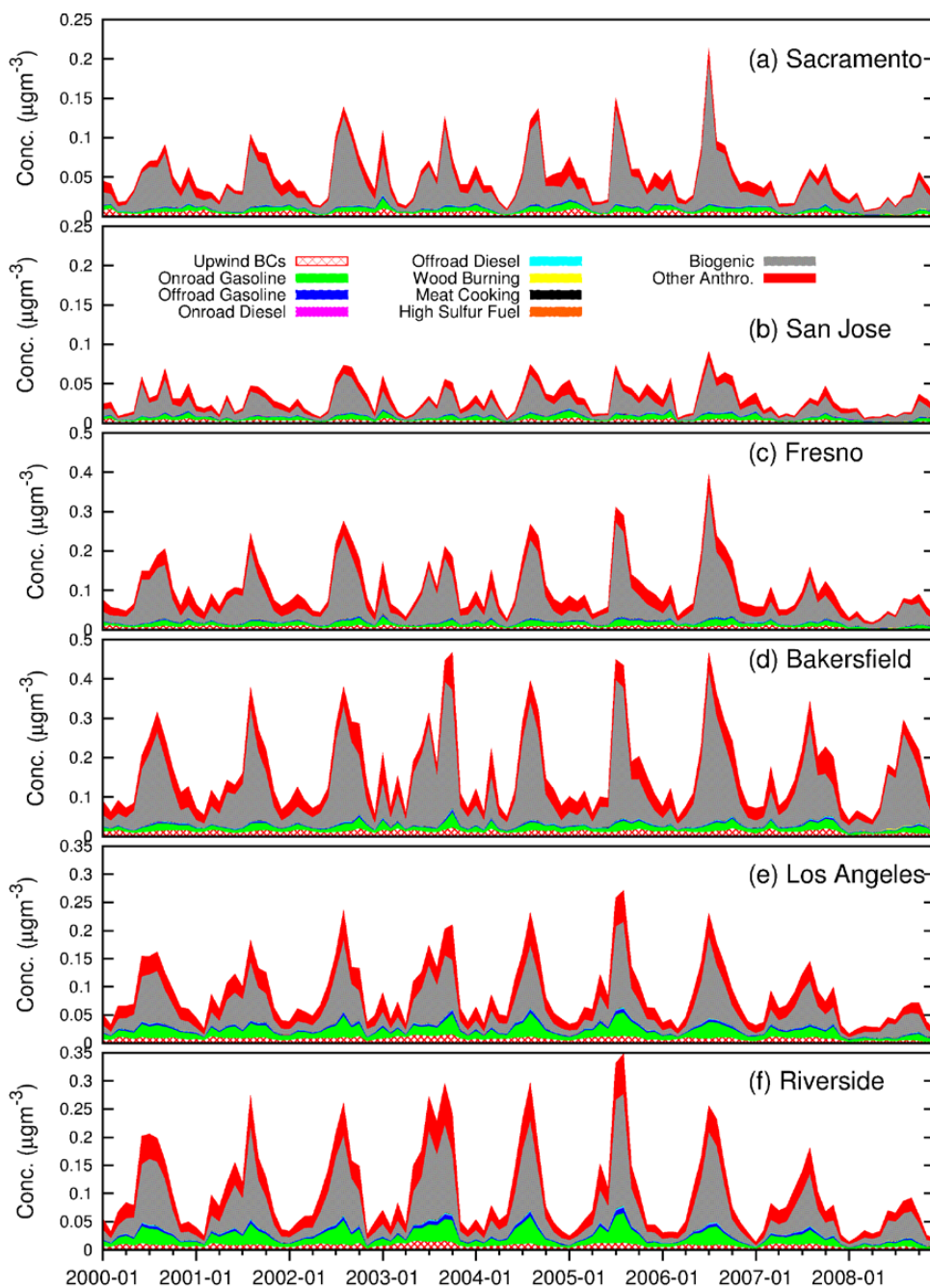
666



667

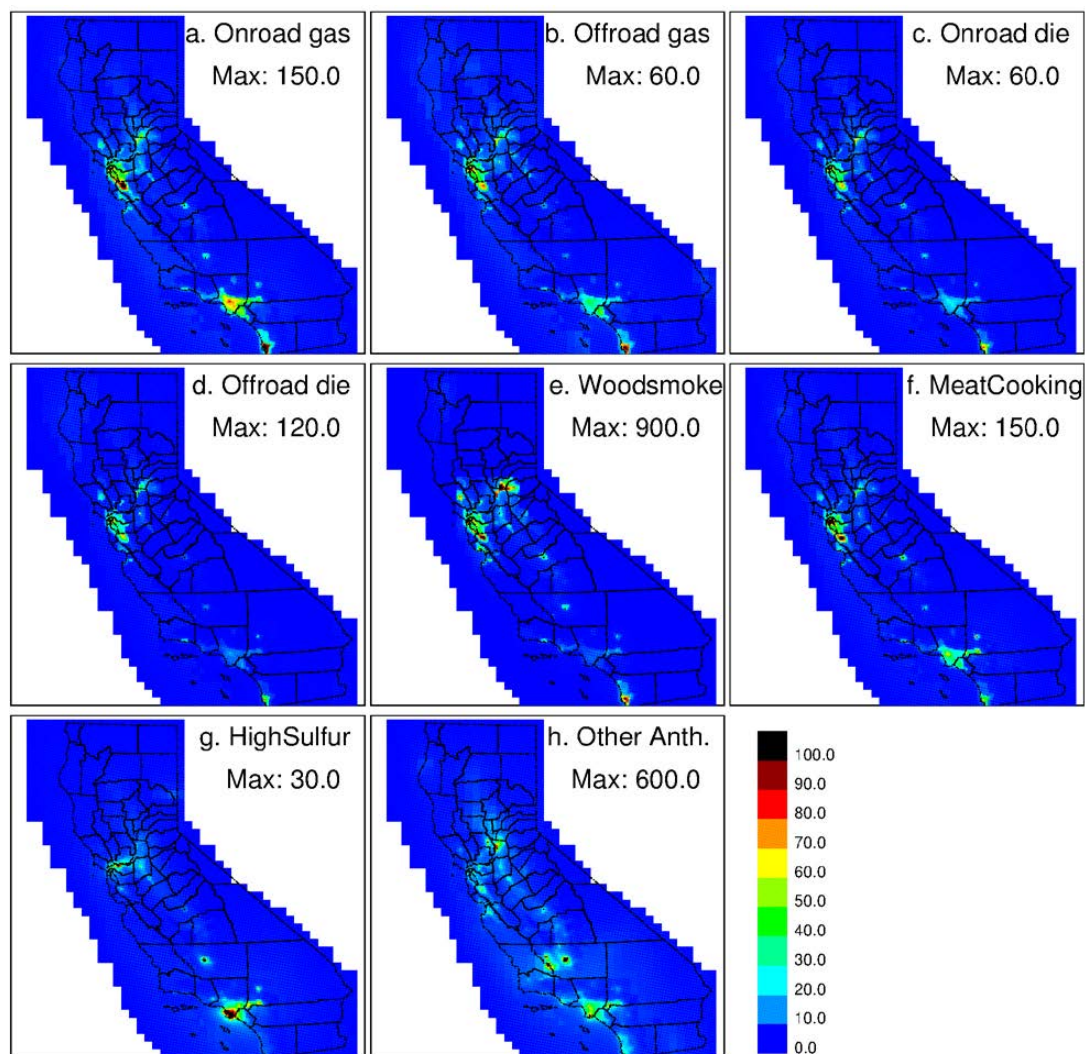
668 Figure 5. The 9-year average $PM_{0.1}$ SOA concentrations derived from (a) AALK, b) AXYL, c)
 669 ATOL, d) ABNZ, e) AISO, f) ATRP, g) ASQT, h) AOLGA, and i) AOLGB. Note AXYL and
 670 ATOL are actually derived from lumped aromatics species ARO2 (groups of aromatics with
 671 $k_{OH} > 2 \times 10^4 \text{ ppm}^{-1} \text{ min}^{-1}$, including xylenes and other di- and polyalkylbenzenes) and ARO1
 672 (groups of aromatics with $k_{OH} < 10^4 \text{ ppm}^{-1} \text{ min}^{-1}$, including toluene and monoalkylbenzenes).
 673 The color scales (shown in the last panel in unit of %) indicate the ratios of the concentrations to
 674 the maximum values, which are shown in the panels under species names with a unit of ng/m^3 .

675



676

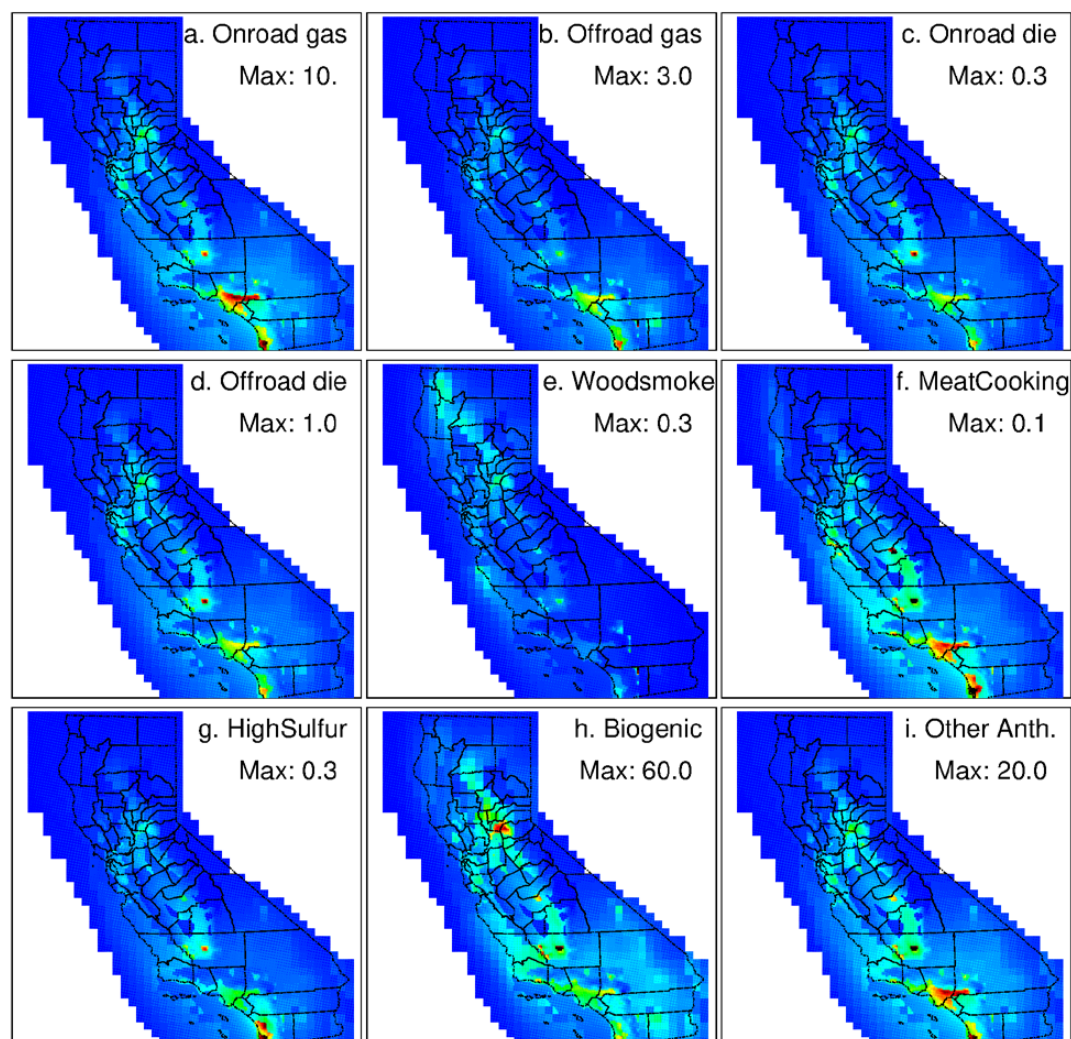
677 Figure 6. Monthly source contributions to $PM_{0.1}$ SOA at 6 urban sites. Predicted $PM_{0.1}$ SOA
 678 concentrations from different sources are indicated by the colored areas.



679

680 Figure 7. Predicted source contributions to 9-year average $PM_{0.1}$ POA concentrations. The color
 681 scales (shown in the last panel in unit of %) indicate the ratio of the concentrations to the
 682 maximum concentration values, which are shown in the panels under source names with a unit of
 683 ng/m^3 .

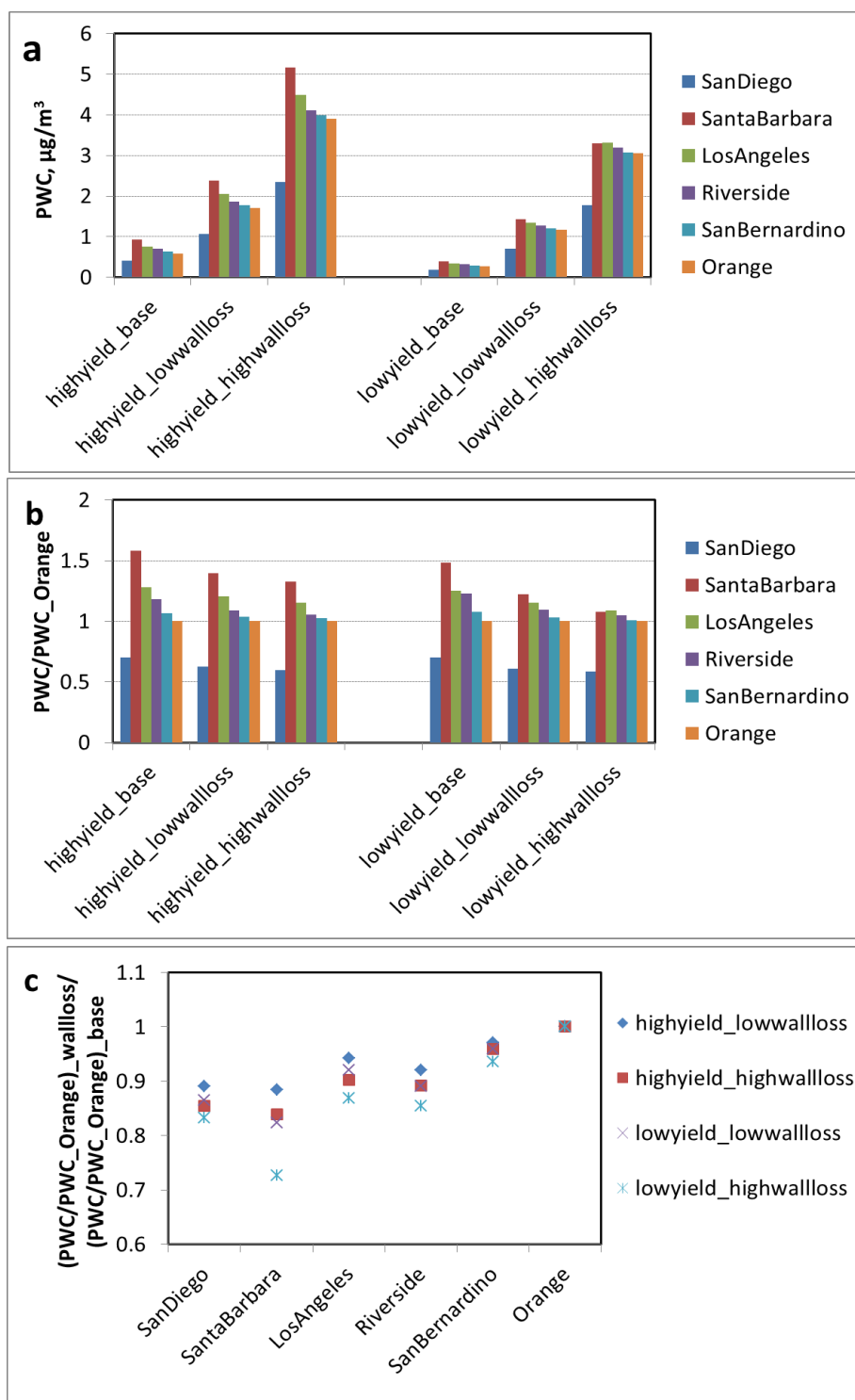
684



685

686 Figure 8. Predicted source contributions to 9-year average $PM_{0.1}$ SOA concentrations. The
 687 definition of the color scales are the same as in Figure 7.

688





690 Figure 9. (a) Predicted population weighted concentrations (PWCs) of SOA in six counties in
691 Southern California. Two sets of simulations (scenarios) conducted by Cappa et al (2015) were
692 used, one with the low-NO_x, high-yield parameters (denoted as “highyield”) and the other with
693 high-NO_x, low-yield parameters (denoted as “lowyield”), and each set of simulations included
694 three vapor wall loss cases, i.e., no considering of vapor wall losses (denoted as “base”), low
695 vapor wall loss rates (denoted as “lowwallloss”), and high vapor wall loss rates (denoted as
696 “highwallloss”). (b) Normalized PWCs of SOA in all counties to the PWC of SOA in Orange
697 County. (c) Changes in the normalized PWCs of SOA in all counties by accounting for vapor
698 wall losses.